Magnetic field controlled reversal of ferroelectric polarization in conical spin ordered multiferroics: Monte Carlo simulation

Xiaoyan Yao (姚晓燕),[1,a)] Veng Cheong Lo (羅永祥),[2] and Jun-Ming Liu (刘俊明)[3]
[1]*Department of Physics, Southeast University, Nanjing 211189, China*
[2]*Department of Applied Physics, The Hong Kong Polytechnic University, Kowloon, Hong Kong*
[3]*Nanjing National Laboratory of Microstructures, Nanjing University, Nanjing 210093, China*

(Received 26 June 2009; accepted 22 August 2009; published online 2 October 2009)

To understand the fascinating multiferroicity observed in $CoCr_2O_4$, Monte Carlo simulation is performed on a three-dimensional spinel lattice with classical Heisenberg spins. The conical spin order is confirmed to be the origin of the peculiar magnetoelectric behavior with coexisting magnetization and ferroelectric polarization. Furthermore, the simultaneous reversals of magnetization and polarization controlled by the external magnetic field are reproduced, consisting with the experimental observation qualitatively. It is revealed that, from the microscopic structures of spins, the axis of spin cone provides a "handle," with which the magnetization and polarization can be reversed by the magnetic field easily. © *2009 American Institute of Physics*.
[doi:10.1063/1.3234401]

I. INTRODUCTION

Multiferroics, especially magnetoelectric (ME) materials, have attracted considerable attention since the 1960s due to their potential applications and fundamental curiosity. In recent years, the magnetism-driven ferroelectricity observed in the frustrated materials renews the interest in this field. Here the frustration plays the role to induce spatial variation in magnetization which breaks the spatial inversion symmetry, and thus produces ferroelectricity.[1] Due to the magnetic origin of ferroelectricity, the ferroelectric behavior in these materials is highly sensitive to the applied magnetic field. Various magnetic controls of ferroelectric behavior have been observed, such as flop,[2] reversal,[3] and rotation[4] of electric polarization. This brings a hopeful prospect for the implementation of diversified electronic devices, such as sensitive magnetic field sensors or magnetic field controlled ferroelectric memories.

The noncollinear spiral spin order is a common way to break the spatial inversion symmetry, and therefore results in ferroelectricity. Different from the ferroelectricity induced by the exchange striction in the collinear spin order,[5–7] the microscopic mechanism of ferroelectricity observed in noncollinear spiral spin order can be explained by the spin current model proposed by Katsura *et al.*,[8] that is, the relation between the local electric polarization (p_{ij}) and the neighboring canting spins (S_i and S_j) is expressed as

$$p_{ij} = -ae_{ij} \times (S_i \times S_j), \tag{1}$$

where e_{ij} denotes the vector connecting the two sites of S_i and S_j, and a is a positive factor determined by the spin exchange coupling and the spin-orbit interaction. This mechanism, also expressed in terms of the inverse Dzyaloshinskii–Moriya interaction,[9] has been used to understood the origin of magnetic ferroelectricity in a lot of compounds, such as $RMnO_3$ (R=Tb and Dy),[2] $MnWO_4$,[10] and $LiCu_2O_2$.[11] But in most of these cases, the ferroelectricity of spiral magnetic origin does not manifest spontaneous magnetization (M). Moreover, the magnetic field required to flip the total polarization (P) is relatively large.

Recently, the fascinating multiferroicity originated from the transverse conical spin order, exhibiting both spontaneous M and P, attracts a lot of interest. It is observed that, in this conical spin state, the spins show the modulated behavior along the chain of magnetic ions. If all the ionic sites in a chain are moved to one site, then the spin vectors will lie on a surface of cone, namely, the spin cone. In other words, all the spins present the homogeneous components along the cone axis, which produce a net M, while the other components of spins rotate in the plane normal to the cone axis along the chain, giving rise to ferroelectricity. As a typical example, this fascinating multiferroicity of conical spin origin has been observed in $CoCr_2O_4$.[12–15] It is revealed in experiments that $CoCr_2O_4$ shows both spontaneous M and P. In particular, P can be easily reversed by the reversal of M during the sweep of magnetic field (h), whichever direction of h is taken as the starting point of sweep. To understand the microscopic mechanism of this fantastic reverse phenomenon, further work should be done.

In this paper, the fascinating multiferroic behavior observed in $CoCr_2O_4$ is investigated by using Monte Carlo simulation based on a model of classical Heisenberg spins in a three-dimensional (3D) spinel structure. It is confirmed that the multiferroic state with coexistence of P and M is realized by the conical spin order in this system. P is always reversed upon the reversal of M during the sweep of h, which is in qualitative agreement with the experimental phenomenon. The microscopic structures of spins under the variation in applied h are discussed to understand the reversal mechanism of P induced by h. It is revealed that the spin rotation axis, namely, the axis of spin cone, provides a "handle," with which M and P can be tuned by h easily.

a)Electronic mail: yaoxiaoyan@gmail.com.

II. MODEL AND SIMULATION

$CoCr_2O_4$, forming crystal in a cubic spinel structure, belongs to a spinel family with the general formula AB_2O_4. Magnetic Co^{2+} and Cr^{3+} ions occupy the tetrahedral (A) and octahedral (B) sites, respectively, and their spin-only values are both $3\mu_B$. Previous investigations indicate that the nearest-neighbor antiferromagnetic A-B and B-B exchange interactions (j_{AB} and j_{BB}) are dominant, and a conical spin state can be induced by these two interactions.[16–18] Considering B-B and A-B nearest-neighbor couplings, a classical Heisenberg exchange energy is given by

$$H = -\sum_{[i,j]} j_{BB} s_{Bi} \cdot s_{Bj} - \sum_{[i,j]} j_{AB} s_{Ai} \cdot s_{Bj}, \tag{2}$$

where s_{Bi} and s_{Ai} are ith classical Heisenberg spin on B and A sites with the same magnitude. $[i,j]$ denotes the summation over all the nearest-neighbor spin pairs. It has been shown in Lyons, Kaplan, Dwight, and Menyuk (LKDM) theory that for a cubic spinel structure the magnetic ground-state structure is determined by the parameter[19,20]

$$u = \frac{4 j_{BB} s_B s_B}{3 j_{AB} s_A s_B}. \tag{3}$$

When $8/9 < u < 1.298$, it was suggested that the ferrimagnetic spiral, namely, the conical spin order, has the lowest energy out of a large set of possible spin configurations. We define the following relatively coupling constants

$$J_{AB} = j_{AB} s_A s_B \quad \text{and} \quad J_{BB} = j_{BB} s_B s_B, \tag{4}$$

and u is then expressed by

$$u = \frac{4 J_{BB}}{3 J_{AB}}. \tag{5}$$

According to the LKDM theory, the ferrimagnetic spiral state is very likely the ground state under the following condition:

$$\frac{2}{3} < \frac{J_{BB}}{J_{AB}} < 0.9735. \tag{6}$$

Therefore we adopt $J_{BB}=-2.5$ and $J_{AB}=-3$ in the present simulation. Considering the magnetic energy and electric energy, the total Hamiltonian can be written as

$$H = -J_{BB} \sum_{[i,j]} S_{Bi} S_{Bj} - J_{AB} \sum_{[i,j]} S_{Ai} S_{Bj} - hM - EP. \tag{7}$$

Corresponding to the coupling constants J_{BB} and J_{AB}, S_{Bi} and S_{Ai} are normalized classic spins, namely, with a magnitude of one. E is the external electric field and M is evaluated by

$$M = \frac{1}{N} \sum_i (S_{Ai} + S_{Bi}), \tag{8}$$

where N is the total number of magnetic ions. P is calculated according to Eq. (1). For convenience, only spin current between spins of B sites is considered. Therefore the total polarization P is expressed as

$$P = \frac{1}{N} \sum_{[i,j]} p_{ij} = -\frac{a}{N} \sum_{[i,j]} e_{ij} \times (S_{Bi} \times S_{Bj}). \tag{9}$$

Since the present simulation is a qualitative investigation on the ME behavior resulting from the conical spin order, a is assumed to be one for convenience.

The Monte Carlo simulation is performed on a 3D spinel lattice composed of classical Heisenberg spins. The system size is $L \times L \times L$ where $L=36$, and the periodic boundary condition is applied. It is assumed that x, y, and z axes are, respectively, along the directions of [100], [010], and [001] in the spinel structure. The spin is updated according to the Metropolis algorithm. Only the low-temperature behaviors at $T=0.01$ are focused. Similar to the ME polarizing procedure in the experiment,[12,15] the system is initially polarized by E and h in simulation. After the ME polarizing process, E is removed, and then M and P are calculated with different h. For every h, the initial 10 000 Monte Carlo steps (MCSs) are discarded for equilibration, and then the results are obtained by averaging 1000 data. Each datum is collected at every 10 MCSs. The final results are calculated by averaging more than 30 independent data sets obtained by selecting different seeds for random number generation.

III. RESULTS AND DISCUSSION

Due to the cubic symmetry and the spin frustration, the states in spinel structure are highly degenerated. In experiments, the ME polarizing procedure is applied to lift the degeneracy of these states, and then produce a single ME domain. Thus the directions of M and P are fixed. For the purpose to compare the simulated results with the experiments conveniently, in the present simulation the electric field of $E=0.7071$ along [110] and magnetic field of $h=1.2$ along [001] are applied to polarize the system. It is worthwhile to note that B sites in the spinel structure are arranged in the rows along [110] or $[1\bar{1}0]$ in the alternate planes normal to z-axis. Accordingly the spins on B sites form chains along [110] or $[1\bar{1}0]$, respectively. As presented in Fig. 1, in order to distinguish these two types of planes, the plane including spin chains along $[1\bar{1}0]$ is donated by P1, and that with chains along [110] is marked by P2. Thus the whole structure of B sites is composed of P1 and P2 stacked alternately along z-axis. As illustrated in Fig. 1, the black arrow shows the projection of spin on xy-plane at the end of ME polarizing procedure. It is seen in Fig. 1(a) that the spin chain in P1 presents a spiral feature along $[1\bar{1}0]$. According to Eq. (1), in P1 along the chain every nearest-neighbor spin pair produces a local polarization p_{ij}. p_{ij} shows a uniform component in P1 along [110] as plotted by blue arrow, while the other components of different p_{ij} counteract with each other. Thus P in the direction of [110] is induced by E along [110]. On the contrary, as presented in Fig. 1(b), there is no spiral along the chains in P2. The nearest-neighbor spins have the same orientations, which induces $p_{ij}=0$. The reason is that the spin chains along [110] cannot result in P along [110] according to Eq. (9). However if E is applied along $[1\bar{1}0]$ in ME polarizing process, the spin spiral will appear

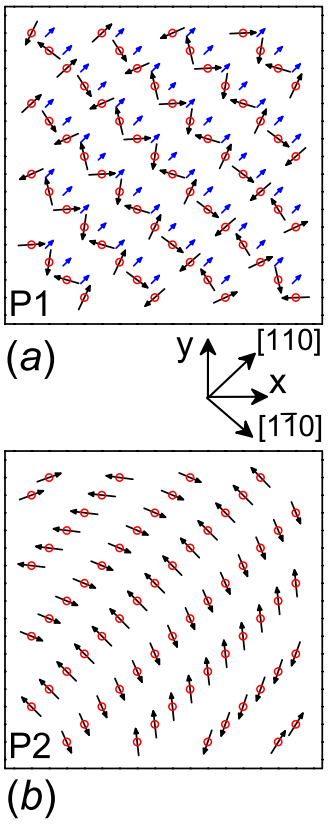

FIG. 1. (Color online) Snapshots for spins of B sites on (a) P1 and (b) P2 projected onto xy-plane at the end of the ME polarizing procedure. The red circle denotes the B site. It is seen that the spin chains are along [1$\bar{1}$0] in P1 and along [110] in P2. The black arrow presents the projection of corresponding spin onto xy-plane. Because the x- and y- components of spin in P2 are too small, they are multiplied by 3 and then plotted in (b). In P1 along the chain, every nearest-neighbor spin pair induces a local polarization p_{ij} whose component in xy-plane is plotted in (a) by the blue arrow.

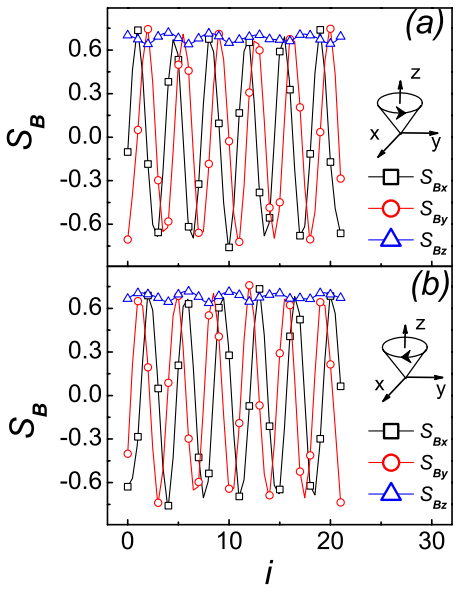

FIG. 2. (Color online) Three components of spins (S_{Bx}, S_{By}, and S_{Bz}) in a chain along [1$\bar{1}$0] in P1 at the end of ME polarizing procedure (a) with E along [110] and (b) with E along [$\bar{1}\bar{1}$0]. The sketch cone inserted in figure demonstrates the rolling direction of spins in the chain.

along [110] in P2 but not in P1. And the spin modulation along [110] will produce P in the direction of [1$\bar{1}$0].

In order to clearly illustrate the spin spiral at the end of ME polarizing procedure, the x-, y-, and z- components of spin on B site (S_{Bx}, S_{By}, and S_{Bz}) in a chain along [1$\bar{1}$0] in P1 are presented in Fig. 2(a). It is seen that S_{Bx} and S_{By} show the behaviors of simple harmonic wave with a phase difference of $\pi/2$, which means that the spin spiral exists in xy-plane. Since h along [001] induces M in the direction of [001], S_{Bz} shows a positive high value. Thus, presented as the sketch in Fig. 2(a), the spins rotate counterclockwise on the surface of a cone with its axis along [001], namely, a conical spin state is produced. This counterclockwise rotation of spin induces the direction of $S_{Bi} \times S_{Bj}$ along [001], and e_{ij} is in the direction of [1$\bar{1}$0], namely, along the chain. According to Eq. (9), P is generated along [110]. If the direction of E is opposite, namely, along [$\bar{1}\bar{1}$0], the phase difference between S_{Bx} and S_{By} will be $-\pi/2$, which means that the spins rotate clockwise, as demonstrated in Fig. 2(b). According to Eq. (9), P is produced along [$\bar{1}\bar{1}$0]. Therefore, the positive or negative value of $\boldsymbol{E}$ induces opposite rotation directions of spins, which lead to P with opposite orientations.

The most interesting behavior observed in $CoCr_2O_4$ is the simultaneous reversal of M and P upon the application of h.[12,15] This behavior is well reproduced in the present simulation. As mentioned above, the ME polarizing process with $E=0.7071$ along [110] and $h=1.2$ along [001] fixes the directions of P and M. Even if E is turned off, P and M remain in the directions of [110] and [001], respectively. That is, M_z, P_x, and P_y show relatively high values, but M_x, M_y, and P_z are about zero. As h along [001] varies between 1.2 and -1.2, M_z, P_x, and P_y all demonstrate hysteretic features, as illustrated in Figs. 3(a) and 3(b). In the branch of h decreasing from 1.2, M_z gradually descends, and then suddenly drops to a negative value at about $h_s=-0.4$. At the same time, P_x and P_y also flop. In the branch of h increasing, M_z, P_x, and P_y flip at about $h_s=0.4$ simultaneously. The error bar shows that the fluctuation is very large for M_z, P_x, and P_y, at the switching point $h_s=0.4$ or -0.4, although the fluctuation is too small to be seen on the other h points. In addition, the values of M_x, M_y, and P_z remain about zero over the whole variation range of h, but the fluctuations of them are relatively high especially near the switching point. If the system is polarized by the opposite h during ME polarizing process, namely, applying $h=-1.2$ along [001] and $E=0.7071$ along [110], and then h is scanned from $h=-1.2$ after E is removed, the simulated results are presented in Figs. 3(c) and 3(d). It is seen that the hysteretic behavior of M_z is the same as Fig. 3(a). P_x and P_y also flip together with M_z, but their curves against h is opposite to Fig. 3(b) due to the different initial polarizing processes and the different starting points of h sweep. It is clearly seen that P is always reversed upon the reversal of M with h increasing or decreasing, which is in agreement with the experimental observation.[12]

In order to understand the reversal of P induced by h, some snapshots of a spin chain along [1$\bar{1}$0] in P1 with h scanning from 1.2 to -1.2 are presented in Fig. 4. In Fig. 4(a), at $h=1.2$ the conical spin order with the counterclockwise rotation is kept even in the absence of E. Thus the

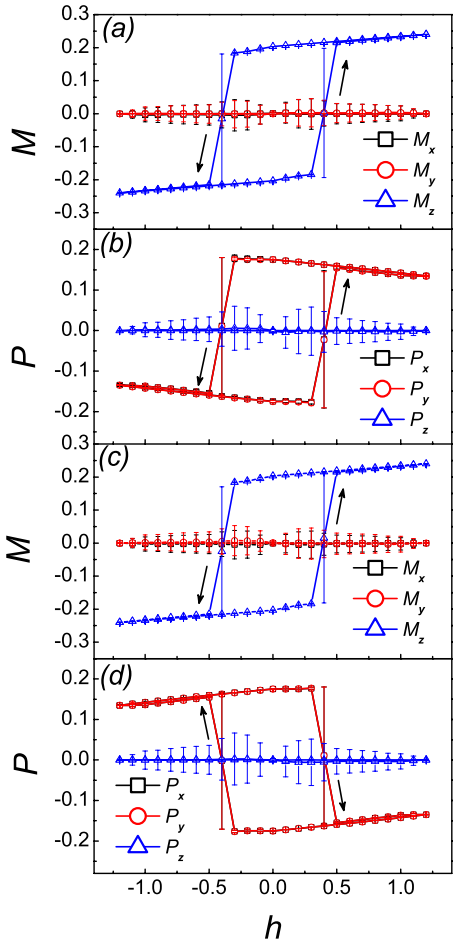

FIG. 3. (Color online) The static hysteretic behaviors of (a) M and (b) P after ME polarizing procedure with $E=0.7071$ along [110] and $h=1.2$ along [001]. Here M_x, M_y, and M_z are three components of M, and P_x, P_y, and P_z are those of P. The static hysteretic behaviors of M and P after ME polarizing process with $E=0.7071$ along [110] and $h=-1.2$ along [001] are presented in (c) and (d), respectively. The fluctuations of M and P are illustrated by error bar.

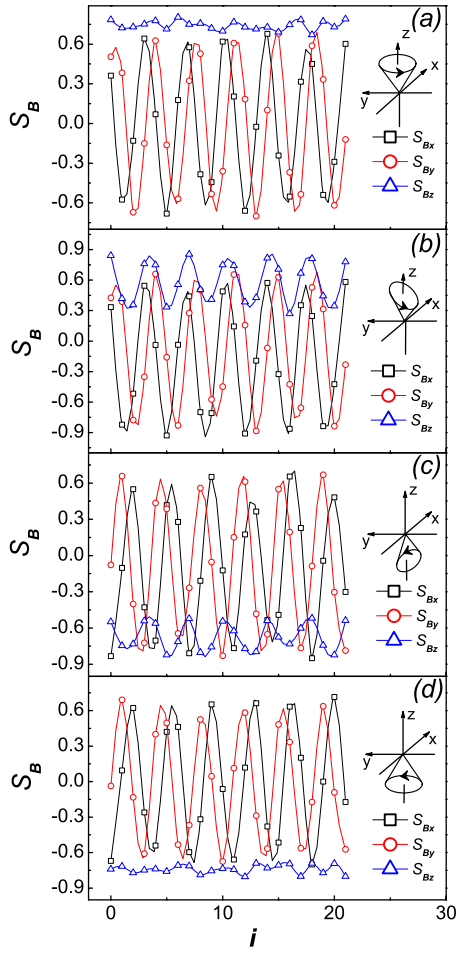

FIG. 4. (Color online) Three components of spins (S_{Bx}, S_{By}, and S_{Bz}) in a chain along $[1\bar{1}0]$ in P1 during the sweep of h along [001] are illustrated in (a) at $h=1.2$, (b) at $h=-0.3$, (c) at $h=-0.5$, and (d) at $h=-1.2$. The sketch cone inserted in the figure demonstrates the rotation direction of spins in the chain.

positive values of M_z, P_x, and P_y remain. As h reaches -0.3, just before the switching point $h_s=-0.4$, S_{Bz} shows a wavelike behavior as demonstrated in Fig. 4(b). Besides, S_{Bx} and S_{By} still hold the wavelike behavior with the phase difference of $\pi/2$, but the whole curves of S_{Bx} and S_{By} shift downward to lower values. The change in S_B implies that the axis of spin cone deviates from [001], namely, the cone slants a little toward $[\bar{1}\bar{1}0]$. After the reversals of M and P, the snapshot of the chain at $h=-0.5$ is demonstrated in Fig. 4(c). It is seen that S_{Bz} flips to negative value, which is responsible for the reversal of M. And the phase difference between S_{Bx} and S_{By} is changed to $-\pi/2$, which means that the spins rotate in the opposite direction, namely, clockwise. Therefore P reverses. In addition, the wavelike behavior of S_{Bz} together with the downward shifts in S_{Bx} and S_{By} curves demonstrates that the axis of spin cone deviates from the direction of $[00\bar{1}]$ and slants a little toward $[\bar{1}\bar{1}0]$. When h decreases to -1.2 as displayed in Fig. 4(d), S_{Bz} shows a waveless figure. S_{Bx} and S_{By} nearly follow the behavior of simple harmonic wave without shifting. All these imply that the spins rotate on the surface of cone with the axis along $[00\bar{1}]$. The complete reversal of spin cone ensures that the values of M and P at $h=-1.2$ have the same magnitude but opposite direction to those at $h=1.2$.

The spin configurations in Fig. 4 indicate that h-controlled synchronized reversals of M and P result from the reversal of spin cone, which is realized by slanting the cone axis in one direction during h sweep. In the process of reversal, the sloping spin cone will produce nonzero values for M_x, M_y, and P_z. However, it is evidenced by simulation that the spin cone may slant from z-axis in any direction, which induces the counteraction of their values. Consequently M_x, M_y, and P_z present the values about zero with the relatively high fluctuation, as shown in Fig. 3. It is worthwhile to note that the rotation direction of spins relative to the cone axis keeps invariable during the reversal of spin cone. If the spin cone is regarded as a whole, the axis of spin cone provides a handle. When h flips the handle, the spin cone is kept unchanged. Thus M and P are reversed by h easily.

IV. CONCLUSION

In summary, the fascinating multiferroicity with coexisting M and P observed in the spinel structure is investigated

by Monte Carlo simulation based on a model of classical Heisenberg spins. It is confirmed that the conical spin order, existing in the low-temperature spinel structure, is responsible for the multiferroic state with coexistent P and M. For such a conical spin state, the inherent M-P coupling can lead to the simultaneous reversals of M and P upon application of h, which is qualitatively consistent with the experimental phenomenon. In order to understand the h-controlled reversal mechanism of P, the microscopic structures of spins under different h are discussed in detail. It is revealed that M and P can be reversed by h easily through reversing the axis of spin cone, while the spin cone is kept unchanged. These simulated results are believed to shed some light on the understanding of the ferroelectricity driven by the conical magnetic order.

ACKNOWLEDGMENTS

This work is supported by the research grants from the National Natural Science Foundation of China (Grant Nos. 10904014 and 50832002).

[1]S.-W. Cheong and M. Mostovoy, Nature Mater. **6**, 13 (2007); K. F. Wang, J.-M. Liu, and Z. F. Ren, Adv. Phys. **58**, 321 (2009).
[2]T. Kimura, T. Goto, H. Shintani, K. Ishizaka, T. Arima, and Y. Tokura, Nature (London) **426**, 55 (2003).
[3]N. Hur, S. Park, P. A. Sharma, J. S. Ahn, S. Guha, and S.-W. Cheong, Nature (London) **429**, 392 (2004).
[4]S. Ishiwata, Y. Taguchi, H. Murakawa, Y. Onose, and Y. Tokura, Science **319**, 1643 (2008).
[5]Y. J. Choi, H. T. Yi, S. Lee, Q. Huang, V. Kiryukhin, and S.-W. Cheong, Phys. Rev. Lett. **100**, 047601 (2008).
[6]X. Yao and V. C. Lo, J. Appl. Phys. **104**, 083919 (2008).
[7]X. Yao, V. C. Lo, and J.-M. Liu, J. Appl. Phys. **105**, 033907 (2009).
[8]H. Katsura, N. Nagaosa, and A. V. Balatsky, Phys. Rev. Lett. **95**, 057205 (2005).
[9]I. A. Sergienko and E. Dagotto, Phys. Rev. B **73**, 094434 (2006).
[10]K. Taniguchi, N. Abe, T. Takenobu, Y. Iwasa, and T. Arima, Phys. Rev. Lett. **97**, 097203 (2006).
[11]S. Park, Y. J. Choi, C. L. Zhang, and S.-W. Cheong, Phys. Rev. Lett. **98**, 057601 (2007).
[12]Y. Yamasaki, S. Miyasaka, Y. Kaneko, J.-P. He, T. Arima, and Y. Tokura, Phys. Rev. Lett. **96**, 207204 (2006).
[13]K. Tomiyasu, J. Fukunaga, and H. Suzuki, Phys. Rev. B **70**, 214434 (2004).
[14]I. Kim, Y. S. Oh, Y. Liu, S. H. Chun, J.-S. Lee, K.-T. Ko, J.-H. Park, J.-H. Chung, and K. H. Kim, Appl. Phys. Lett. **94**, 042505 (2009).
[15]Y. J. Choi, J. Okamoto, D. J. Huang, K. S. Chao, H. J. Lin, C. T. Chen, M. van Veenendaal, T. A. Kaplan, and S.-W. Cheong, Phys. Rev. Lett. **102**, 067601 (2009).
[16]G. Lawes, B. Melot, K. Page, C. Ederer, M. A. Hayward, T. Proffen, and R. Seshadri, Phys. Rev. B **74**, 024413 (2006).
[17]C. Ederer and M. Komelj, Phys. Rev. B **76**, 064409 (2007).
[18]T. A. Kaplan, K. Dwight, D. Lyons, and N. Menyuk, J. Appl. Phys. **32**, S13 (1961).
[19]T. A. Kaplan, Phys. Rev. **119**, 1460 (1960).
[20]D. H. Lyons, T. A. Kaplan, K. Dwight, and N. Menyuk, Phys. Rev. **126**, 540 (1962).